ELSEVIER

Biophysical Chemistry 70 (1998) 75–85

Biophysical Chemistry

# Vesicular membrane permeability of monomethylarsonic and dimethylarsinic acids

R.G. Males [a], J.C. Nelson [a], P.S. Phillips [a], W.R. Cullen [a], F.G. Herring [b,*]

[a] *University of British Columbia, 2036 Main Mall, Vancouver, BC, Canada V6T 1Z1*

[b] *Department of Chemistry, University of British Columbia, 2036 Main Mall, Vancouver, BC, Canada V6T 1Z1*

Received 27 March 1997; revised 28 August 1997; accepted 28 August 1997

**Abstract**

The transmembrane permeability coefficients of the environmentally sensitive arsenicals, monomethylarsonic acid (MMA) and dimethylarsinic acid (DMA) have been measured for egg phosphatidylcholine large unilamellar vesicles. The determination of the vesicle concentration-independent first-order rate constants for membrane transport and the permeability coefficients were made using an NMR technique employing shift agents. The permeability coefficient of DMA was found to be two orders of magnitude greater than that of MMA. This is attributed to the presence of MMAs extra hydroxyl group. Both species are shown to permeate membranes in the neutral form. Both the temperature dependence and the dependence on cholesterol content were investigated for DMA. The activation energy and the Arrhenius preexponential factor were found to be dependent on the cholesterol content. A marked increase in both parameters was observed up to 20 mol.% cholesterol, with a further, small increase up to 60%. The significance of these results to our understanding of membrane transport is discussed. The importance of using permeability coefficients rather than *n*-octanol/water partition coefficients in determining bioavailability and bioaccumulation of environmentally sensitive compounds is also discussed. © 1998 Elsevier Science B.V.

*Keywords:* Nuclear magnetic resonance; Phosphatidylcholine membranes; Transport; Cholesterol; Dimethylarsinic acid; Monomethylarsonic acid

## 1. Introduction

The most important function of any biological membrane is to serve as a general diffusion barrier, and it is well known that the lipid bilayer is responsible for this. Lipid bilayers do not act as absolute permeation barriers since, in the absence of carriers, they allow the passage of various types of small molecules at finite rates. Thus, it is by studying the permeability properties of the membrane that a better understanding of this barrier can be obtained. Such studies have been carried out extensively with biological membranes, and more recently with model membranes [1–3]. These studies were mostly concerned with the changes in the rate of permeation in a given membrane system, when the nature of the solute was altered. The analysis of the results showed that the permeation rate was determined primarily by the hydrophobicity of the solute, suggesting that the solute must first dissolve in the interior of the membrane in order for permeation to occur [4,5].

* Corresponding author.


*PII* S0301-4622(97)00108-7

Also of importance is the changes in permeability properties of membranes composed of different lipids, in view of the wide variety of lipid species produced by various organisms. Although progress has been made [6,7], such comparative studies are limited in number, in part due to the technical difficulty in performing such experiments. It is known, however, that passive permeability increases steeply if the lipid environment is too fluid, or if the temperature is too far above the lipid thermal transition temperature [8]. Recent interest in fatty and bile acids [9,10], cancer therapy [11], and environmental issues [12,13] has led to an increased attention to the problems of membrane transport.

The transport of biohazardous molecules across membranes has important environmental consequences. A conventional measurement of the ability of a compound to cross a membrane and to bioaccumulate is the *n*-octanol/water partition coefficient [14]. For example, Neely et al. [15] have shown that the uptake of chlorobenzenes and chlorophenols into trout muscles correlates linearly with their *n*-octanol/water partition coefficients. This correlation is generally used because many of the organic compounds that are known or suspected to constitute a hazard to the environment are highly lipid soluble and, therefore, have relatively large partition coefficients [16]. These compounds also usually exist as a single molecular species in the environment and do not possess ionizable groups. By definition, a partition coefficient is the distribution of a single molecular species between the two phases being considered [17].

Although *n*-octanol/water partition coefficients can be measured directly, they may have limited value in predicting relative permeability coefficients if the domain probed in partitioning studies is not the rate-limiting domain for transport. Lipid bilayers are heterogeneous systems that can be divided roughly into three regions: a highly ordered, highly polar head group region, an ordered hydrocarbon chain region near the head group region, and a region of relatively high disorder at the center of the membrane. Each region has its own physico-chemical and diffusion properties [18]. Since lipid bilayers are heterogeneous systems, difficulties in interpreting partition coefficients arise for solutes that are weak electrolytes, as their activity in each region may be different. Further difficulties arise because hydrophilic compounds partition very poorly into *n*-octanol, making it difficult to correlate partition coefficients with bioaccumulation. This is particularly evident when the environmental impact of arsenic compounds is considered.

Arsenic is present in the environment in a wide variety of different chemical forms [19], and although it occurs naturally, it is also introduced through use as herbicides and as a by-product of a number of industrial processes. Each of its different chemical forms possess different physical and chemical properties, toxicities, mobilities, etc. and it is only when these are known that the arsenic biogeochemical cycle can be fully understood.

Dimethylarsinic acid (DMA) is a widely used pesticide and an important intermediate in the marine biocycling of arsenic. There are considerable differences in the uptake of DMA and monomethyl arsonic acid (MMA) by unicellular algae. When grown in a medium containing 2 ppm DMA, *Isochrisis galbana* accumulated 76% of the available arsenic [20]. From media containing 1 ppm and 5 ppm MMA, the same cellular concentration of *I. galbana* accumulated 25% of the available arsenic. Likewise, *Dunaliella tertiolecta* accumulated 50% of DMA from media containing 0.5 ppm of the appropriate arsenical.

It is possible that the differences between DMA and MMA described above are simply due to differences in the initial rates of diffusion of these compounds into the cell. In fact, Cullen et al. [21] have shown that arsenate is taken up by Chumicola via an active transport mechanism; whereas arsenite, MMA, and DMA appear to enter the cell mainly by passive diffusion processes. The *n*-octanol/water partition coefficients for MMA and DMA are known [22] and are very similar; thus, the differing uptakes cannot be accounted for on this basis. As an alternate to the use of partition coefficients to assess the bioaccumulation and biomobility, we suggest that the permeability coefficients for these types of molecules can be better correlated to their biological behavior.

This notion is tested by determining the permeability coefficients for DMA and MMA using extruded large unilamellar vesicles (LUVs). A discussion of the permeation of both lipophilic and lipophobic permeants across the membranes of LUVs

has been presented earlier [23], forming the theoretical basis of any technique chosen. The permeability coefficients of molecules can be measured with a variety of techniques, the most common of which is radiolabeling. The work presented here describes the determination of permeability coefficients using an NMR technique that has been described earlier [24] and recently reviewed [25]. This study contributes to our understanding diffusive transport of weak lipophobic electrolytes across bilayer membranes.

## 2. Materials and methods

LUVs were prepared by the extrusion procedure of Hope et al. [26] and Mayer et al. [27]. A 1.5-ml solution of DMA or MMA (40 mg $ml^{-1}$) and 300 mM *N*-2-hydroxyethylpiperazine-*N'*-2-ethanesulfonic acid (HEPES) buffer in $D_2O$ was adjusted with NaOH or HCl to the desired pH as monitored by a pH meter. The p$K'$s of DMA and MMA were determined by NMR to be constant over the temperature range employed. This solution was used to hydrate 0.3 g of a mixture of dried egg phosphatidylcholine (Northern Lipids, Vancouver, BC, Canada) and cholesterol (Sigma Chemical, St. Louis, MO). The mixture was vortexed to produce a multilamellar suspension. This suspension was frozen in liquid nitrogen and thawed in warm water (40°C) five times to increase the bilayer unilamellarity [26]. This freeze-thawed suspension was transferred into an extruder (Lipex Biomembranes, Vancouver, BC, Canada) and passed, 10 times, through two 200-nm pore size polycarbonate filters (Nucleopore Canada, Toronto, ON, Canada) under 600 psi nitrogen gas to produce LUVs. A concentration gradient was imposed across the LUV membranes by eluting 0.5 ml of the vesicle suspension down a Sephadex G-50 (Pharmacia Fine Chemicals, Uppsala, Sweden) column (1.5 × 5 cm) with a 40 mM HEPES solution in $H_2O$.

In a typical experiment, 0.4 ml of the post column LUVs were added to an NMR tube containing 10 $\mu$l of 45 mM 3-(trimethylsilyl)-1-propane sulfonic acid (DSS) in $D_2O$ as a chemical shift reference, 20 $\mu$l of 30 mM manganese sulfate in $D_2O$ as a shift reagent, and 170 $\mu$l of 40 mM HEPES buffer solution in $D_2O$. The deuterated buffer was required to provide a $^2H$ lock signal. To preserve the isotonicity of the system, 30 mg of $\alpha$-D(+)-glucose was also added. Successive $^1H$ NMR spectra were accumulated in an automated fashion with a Bruker AM400 NMR spectrometer using quadrature detection. The temperature was controlled with a BVT-100 temperature controller. Each spectrum resulted from 2 dummy scans followed by 8 scans of 4096 data points, 2 s water presaturation, a 90° detection pulse, and a 5200 Hz sweep width (TR = 4 s). Peak areas of the internal and external DMA or MMA resonances were analyzed using the deconvolution routine in the Bruker WIN-NMR program (version 940401). To account for time-dependent spectrometer fluctuations, the areas of the inner and outer peaks were standardized with the area of a reference peak such as DSS or a buffer peak. Alternatively, since the amount of the hydrophilic permeant resident within the membrane is minimal, the areas of each of the two resonances could be divided by their sum, a constant in time. Both methods of standardization produced the same results, giving the standardized peak areas, $I_i$ and $I_o$ (see Eqs. (1) and (2)).

Aliquots of the post-column LUV suspension were assayed for lipid phosphorus using traditional techniques [28]. The vesicle surface area ($A_{mem}$) of the suspension could then be calculated assuming that the inner ($A_i$) and outer ($A_o$) membrane surface areas were equal, $A_o = A_i = A_{mem}$, and that the surface area per phospholipid molecule was 60 $Å^2$.

## 3. Analysis and results

The vesicle system is described in terms of the four compartment model [23,29] illustrated in Fig. 1.

A scheme for the transport of a monoprotic acid responding to an imposed concentration gradient may be represented by:

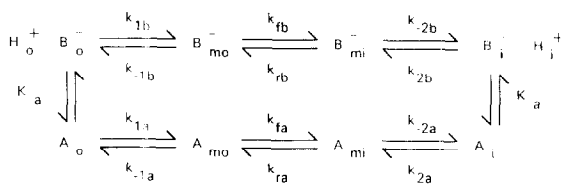


where A represents the neutral acid and B is its anionic conjugate base. The outer and inner aqueous

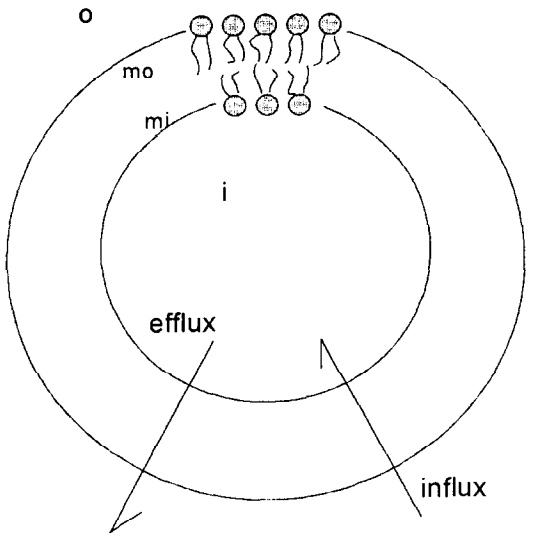


Fig. 1. Large unilamellar vesicle (LUV) showing the four regions occupied by the molecules: the outer aqueous solution (o), the external membranous region (mo), the internal membranous region (mi), and the inner aqueous solution (i). The arrow-labeled efflux depicts an experiment with the bulk of permeant trapped inside the vesicle at time $t = 0$. The arrow-labeled influx depicts an experiment with the bulk of permeant outside the vesicle at $t = 0$.

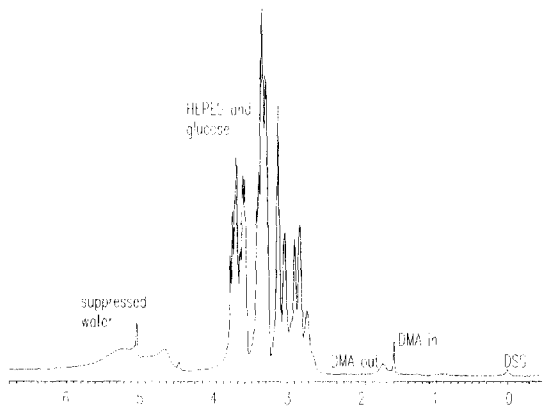


Fig. 2. The water-suppressed 400 MHz $^1$H NMR spectrum of DMA inside and outside of large unilamellar vesicles. The external DMA signal has been shifted and broadened by $Mn^{2+}$.

regions are denoted o an i, respectively. The outer membranous region is represented by mo with the inner membranous region represented by mi. The dissociation of the acid in aqueous solution is $K_a$ ($K_a = 5.2 \times 10^{-7}$ for DMA [22]). The remaining constants of the above scheme have been described previously [23]. This scheme assumes that proton leakage through the membrane is minimal, and that acid dissociation within the membranous regions is negligible.

A typical water suppressed $^1$H NMR spectrum of the vesicle system is illustrated in Fig. 2. The neutral and anionic forms of DMA comprise the composite NMR signal, the area ($I$) of which is proportional to the total number of neutral and anionic DMA molecules ($N$). Inner and outer aqueous DMA resonances are resolved through the addition of $Mn^{2+}$ to the outer aqueous region of the system. Although $Mn^{2+}$ is observed to broaden the outer signal, the induced chemical shift made its use amenable. The time dependence, due to passive efflux, of the areas of these signals, has been previously derived [23]:

$$I_o(t) = I_o^{eq} + \left(I_o^0 - I_o^{eq}\right)\exp\left[-\gamma(t - t_o)\right] \quad (1)$$

$$I_i(t) = I_i^{eq} + \left(I_i^0 - I_i^{eq}\right)\exp\left[-\gamma(t - t_o)\right] \quad (2)$$

where $\gamma$ ($s^{-1}$) is defined as:

$$\gamma = \frac{P_1 A_o}{R_o V_o} + \frac{P_2 A_i}{R_i V_i} \quad (3)$$

$I^0$ is the area of the signal at $t = t_0$, the time the first FID is collected after imposition of the concentration gradient. $I^{eq}$ is the area of the signal when the system has reached equilibrium. For DMA in the pH range 7.0–8.0, equilibrium is usually reached in less than 24 h. $A_o$ and $A_i$ are the outer and inner surface areas of the vesicles, respectively. For LUVs 200 nm in diameter, $A_o \approx A_i$ and will be referred to as $A_{mem}$. $V_o$ and $V_i$ are the volumes of the outside and

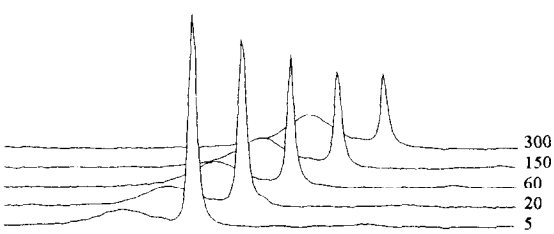


Fig. 3. Inner and outer DMA signals as a function of time after imposition of concentration gradient by elution of vesicles down Sephadex column. Times shown on left are in minutes.

inside aqueous compartments, and may be considered time-independent under isotonic conditions. $P_1$ is the pH-dependent permeability coefficient for inward transport through the bilayer, and $P_2$ is that for outward transport. Since no pH gradients were imposed in these experiments, $P_1 = P_2 = P$ (m s$^{-1}$). $P$ is defined as

$$P = P_a \alpha + P_b(1 - \alpha) \quad (4)$$

where $P_a$ and $P_b$ are the pH-independent permeabil-

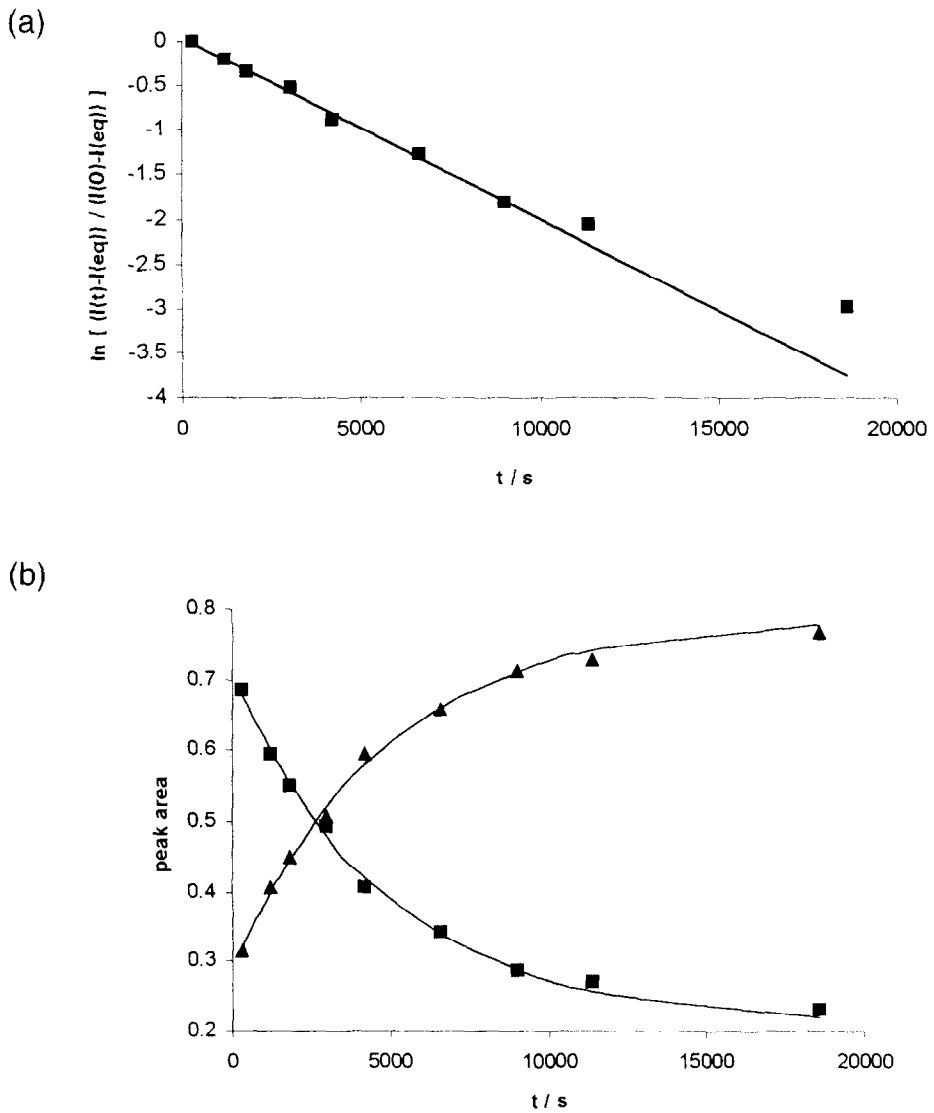


Fig. 4. (a) Semilog plot for inner DMA peak from efflux experiment at pH 7.4 and 298 K. $I(0)$ represents the peak area at $t = 0$, the time that the first FID was obtained. The squares (■) represent observed data, while the line represents the linear regression fit ($R^2 = 0.976$). (b) Relative peak areas obtained by deconvolution of inner (■) and outer (▲) DMA peaks from efflux experiment at pH 7.4 and 298 K. The lines represent the fits obtained from the linear regression performed on the data in (a). Error in peak area is ±5%.

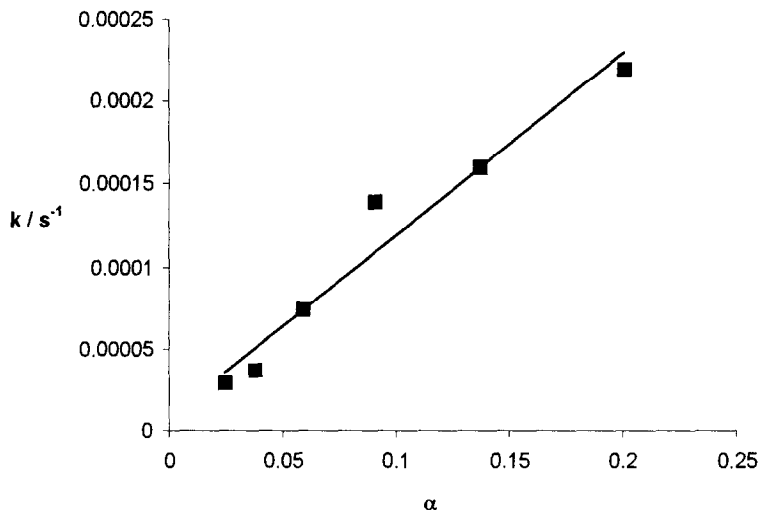


Fig. 5. Effect of pH (and therefore $\alpha$) on the apparent rate constant of permeation, $k$ ($s^{-1}$). The squares represent observed data points and the line represents linear regression analysis. A slope of $1.1 \times 10^{-3}$ $s^{-1}$ and intercept of $8.7 \times 10^{-6}$ were obtained ($R^2 = 0.951$).

ity coefficients of the neutral acid and anionic base, respectively. The extent of acid dissociation ($\alpha$) in the aqueous regions is $\alpha = [H^+]/([H^+] + K_a)$. $R_o$ and $R_i$ are defined as

$$R_o = 1 + \frac{K^* V_{mo}}{V_o} \quad (5)$$

$$R_i = 1 + \frac{K^* V_{mi}}{V_i} \quad (6)$$

$V_{mo}$ is the volume of the outer membranous region and $V_{mi}$ is that of the inner region. $K^*$ is the apparent partition coefficient [23]. DMA ($K^* = 8.4 \times 10^{-3}$ at pH 7.0[22]) is sufficiently hydrophilic that

Table 1
pH effect on the permeation of DMA through phospholipid vesicles

| pH | $k$ ($1 \times 10^{-4}$ $s^{-1}$) | $P$ ($1 \times 10^{-11}$ m $s^{-1}$) |
|---|---|---|
| 7.0 | 2.2 | 1.5 |
| 7.2 | 1.6 | 1.1 |
| 7.4 | 1.4 | 1.2 |
| 7.6 | 0.74 | 0.36 |
| 7.8 | 0.37 | 0.23 |
| 8.0 | 0.29 | 0.21 |

The average standard deviation for $k$ represented about 6.3% of its value.

$K^* V_{mo} \ll V_o$ and $K^* V_{mi} \ll V_i$ hence, $R_o \approx R_i \approx 1$. $\gamma$ may now be simplified to:

$$\gamma = \frac{PA_{mem}}{V_i}\left(1 + \frac{V_i}{V_o}\right) = k\left(1 + \frac{V_i}{V_o}\right) \quad (7)$$

where $k$ is a pH-dependent rate constant that is independent of the concentration of the vesicles. $V_i/V_o$ is determined from the equilibrium spectrum where it is equal to $I_i^{eq}/I_o^{eq}$. The pH dependence is similar to that of the permeability coefficient of Eq. (4):

$$k = k_a\alpha + k_b(1 - \alpha) \quad (8)$$

A series of proton spectra of the permeant DMA as a function of time after column elution are shown in Fig. 3. The inside peak is decreasing in intensity while the $Mn^{2+}$ shifted and broadened outside peak is increasing with time. To evaluate $\gamma$, least squares analyses of semilog plots such as · · · depicted in Fig. 4(a) were performed within the first half-life resulting in curve fits such as those displayed in Fig. 4(b).

From $\gamma$, the vesicle concentration independent rate constant ($k$) can be calculated. In accordance with Eq. (8), a plot of $k$ vs. $\alpha$ results in a straight line of slope $k_a - k_b$ and intercept $k_b$. The $k$ vs. $\alpha$ plot for DMA at 298 K is illustrated in Fig. 5. A

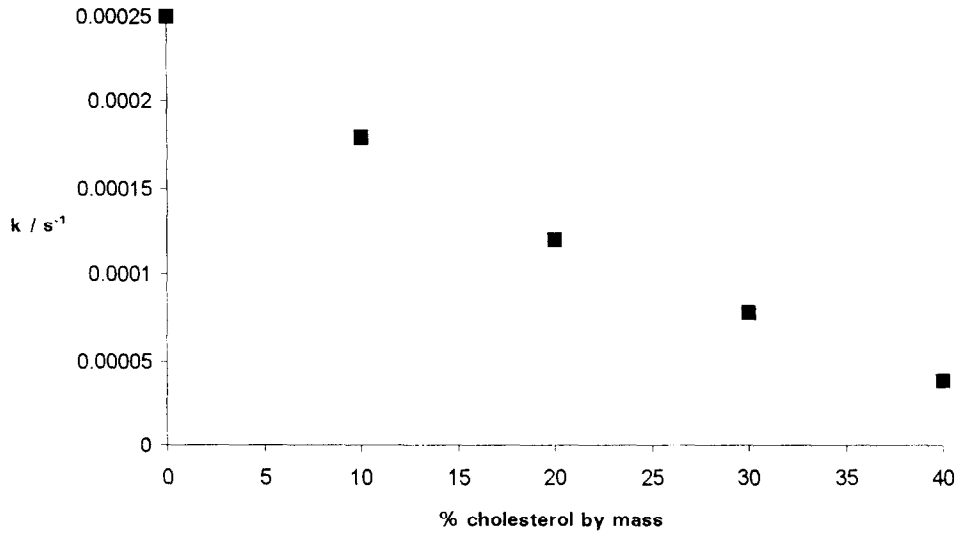


Fig. 6. Effect of cholesterol on the DMA efflux rate constant, $k$, at pH 7.4 and 303 K.

pH-independent rate constant of $k_a = 1 \times 10^{-3}$ s$^{-1}$ was obtained for the neutral form of DMA. As judged by the magnitude of the intercept, the anionic base permeates with a rate constant approximately 2 orders of magnitude slower than the neutral acid.

Knowledge of $A_{mem}$ and $V_i$ permits calculation of the pH-dependent permeability coefficient, $P$, from $k$ using Eq. (7). The surface area $A_{mem}$ was determined from the phosphorus assay with typical values ranging from 2 to 4 m$^2$ per ml of vesicle suspension. Assuming $V_{mi}$ and $V_{mo} \ll V_i$ and $V_o$, calculation of $V_i$ is straightforward, since the total volume of the system is fixed at 600 $\mu$l. Table 1 contains values of pH-dependent rate constants and permeability coefficients for DMA permeating cholesterol free vesicles at 298 K.

A plot of $P$ vs. $\alpha$ analogous to that in Fig. 5 was produced, yielding a pH-independent permeability

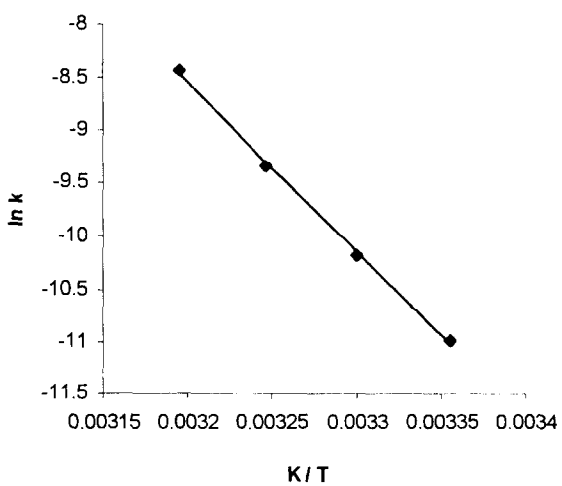


Fig. 7. Arrhenius plot of DMA efflux rate constant, $k$, at pH 7.4. Membranes contained 40% cholesterol by mass. $R^2 = 0.998$.

Table 2
Arrhenius parameters obtained from temperature variation of DMA efflux experiments

| Mass % cholesterol | Mol.% | ln $A$ | $E_a$ (kJ mol$^{-1}$) |
|---|---|---|---|
| 0 | 0 | 24.6 | 76.5 |
| 10 | 18 | 39.2 | 115 |
| 20 | 34 | 39.1 | 115 |
| 30 | 47 | 42.2 | 125 |
| 40 | 58 | 44.7 | 132 |

Standard deviations of 0.1 for ln $A$ and 1000 K for $E_a/R$ were observed.

coefficient $P_a = 8 \times 10^{-11}$ m s$^{-1}$ for neutral DMA, with the anion permeating about two orders of magnitude slower.

The effect of membrane composition on the permeability of DMA was investigated by the addition of varying amounts of cholesterol to the lipids used to form the LUVs. The effect of cholesterol on the rate constant for permeation of neutral DMA at constant temperature is illustrated in Fig. 6. Experiments were also carried out at various temperatures and cholesterol composition. The rate constant for permeation exhibited a typical Arrhenius behaviour as illustrated in Fig. 7. The Arrhenius parameters exhibited a dependence on membrane composition. The results are summarized in Table 2.

The analysis for a monoprotic acid may easily be extended to treat diprotic acids such as MMA. $I_0$ and $I_i$ in Eqs. (1) and (2) will now represent the areas of the composite NMR signals comprised of the neutral acid, monoanionic, and dianionic forms of MMA. As with DMA, MMA is also sufficiently hydrophilic ($K^* = 7.4 \times 10^{-3}$ at pH = 7.0[22]) that $R_0 \approx R_i \approx 1$ in Eqs. (5) and (6). $P$ in Eq. (7) hence becomes:

$$P = P_a\alpha + P_b\alpha\frac{K_1}{[H^+]} + P_c\alpha\frac{K_1K_2}{[H^+]^2} \qquad (9)$$

$P_c$ is the permeability coefficient of the dianionic base. $K_1$ ($7.8 \times 10^{-5}$) is the acid dissociation constant for neutral MMA and $K_2$ ($1.7 \times 10^{-9}$) is the dissociation constant for monoanionic MMA [22]. In Eq. (9), $\alpha = [H^+]^2/([H^+]^2 + K_1[H^+] + K_1K_2)$.

Permeabilities, $P$, of $7 \times 10^{-13}$ and $3 \times 10^{-13}$ m s$^{-1}$ were observed for MMA passing through cholesterol free vesicles at pH 7.0 and 7.4, respectively. From this pH dependence, it was calculated that the permeability coefficient of the diprotic (neutral) acid is approximately $P_a = 5 \times 10^{-13}$ m s$^{-1}$ while the monoanion and dianion permeate at least 4 orders of magnitude slower. Since the approach to equilibrium of the MMA/cholesterol-free LUV system takes several days, experiments with cholesterol-loaded vesicles were not performed.

## 4. Discussion

We have studied the effects of pH, temperature and membrane composition on the rates of passive efflux of DMA and MMA. Using a kinetic model previously derived [23], permeation rate constants independent of vesicle concentration were calculated from the two distinct resonances of the permeant inside and outside the vesicles. Using the vesicle surface area as determined from phosphorus assays, permeability coefficients were then calculated.

The observation that the rate constant, $k$, increases with decreasing pH, as illustrated in Fig. 5, is consistent with DMA preferentially diffusing through the membrane in its neutral form. The data obtained obey the predicted dependence on $\alpha$ in Eq. (8). The rate constant of $k_a = 1 \times 10^{-3}$ s$^{-1}$ was obtained for permeation of protonated DMA. This rate constant translates into a permeability coefficient for the neutral species of $P_a = 8 \times 10^{-11}$ m s$^{-1}$. The rate constant for permeation of the anionic form may, in principle, be calculated from the $y$-intercept of the $k$ vs. $\alpha$ plot. Since the intercept in Fig. 5 is small with respect to its standard deviation, we are not able to quote an anionic rate constant with accuracy. We can, however, approximate that permeation of the anion occurs 100 times slower than the neutral species. The permeation of neutral diprotic MMA was calculated to occur with a permeability coefficient of $P_a = 5 \times 10^{-13}$ m s$^{-1}$, while the monoanionic form of MMA permeated at least 4 orders of magnitude slower.

The observation that the neutral forms of weak acids and bases permeate faster than the anionic forms is in accordance with reports by several others [11,24,30]. For example, maleic acid is reported to traverse egg phosphatidylcholine (EPC) bilayers with a permeation coefficient 4 orders of magnitude faster

than maleate monoanion [24]. Since the rate constants for the permeation of neutral ($k_a$) and charged ($k_b$) DMA implicitly contain partition coefficients, this result is expected, as ions do not partition into lipophilic media as well as do neutral species [17].

The difference in rates of permeation of MMA and DMA may be attributed to their differences in chemical groupings. According to Stein [31], every hydroxyl group that is added to a molecule may be expected to decrease its permeability 100- or 1000-fold. Conversely, every methyl group added is likely to increase permeability 5-fold. The structural difference in going from DMA to MMA being the substitution of a hydroxyl for a methyl group is therefore consistent with the observed 100-fold increase in the permeability coefficient of DMA over MMA.

Early studies on the effect of cholesterol incorporation into cell and model membranes showed that it reduced permeability of some nonelectrolytes [8,32–37]. McElhaney et al. [33] reported that activation energy values for the overall permeation process were not significantly affected by variation in cholesterol content. Deuticke and Ruska [34] observed that a pronounced reduction in the permeability of nonelectrolytes in erythrocytes took place up to 40 mol.% cholesterol. Permeability was affected only slightly in cells with a cholesterol content higher than this. Recent studies by Nouri-Sorkhabi et al. [36] and Waldeck et al. [37] have shown that increases in cholesterol may result in decreases in the permeability of human erythrocytes . It has been observed that cholesterol decreases lateral diffusion in model and cell membranes, resulting in decreased fluidity of the membranous region [38–40]. A recent molecular dynamics study [41] concurs, suggesting that cholesterol causes an increase in the motional ordering of the phospholipid chains, resulting in a decrease in the kink [42] population.

There is a consistent decrease in the rate of permeation of DMA with increasing cholesterol incorporation into the membrane as illustrated in Fig. 6. This decrease in permeability is consistent with the previous reports [8,32–37]. Since the rate constant of permeation measured here intrinsically contains the effect of partitioning into the membrane, i.e., we have measured $k = PA_{mem}/V_i$ (see Eq. (7)) where the permeability coefficient, $P = KD_{mem}/\delta r$, is by definition a function of the partition coefficient ($K$), the diffusion coefficient within the membrane ($D_{mem}$), and the width of the membrane ($\delta r$). Hence, if one considers the rate constant $k$ to be a function of the partition coefficient and of a constant of membrane permeation ($k_{mem}$) such that $k = Kk_{mem}$, then $k_{mem} = D_{mem} A_{mem}/\delta r V_i$.

A recent study by Subczynski et al. [43] on the effect of cholesterol on hydrophobic barriers of lipid bilayer membranes provides a basis for the interpretation of our results. They showed that in EPC membranes, similar to those used in the present study, the effects of cholesterol are: (a) to increase the extent of penetration of water and ions into the polar headgroup region and the near-surface region of the hydrocarbon phase (up to acyl position 10), and, (b) increase sharply the hydrophobic barrier in the hydrocarbon phase after this near-surface region. Therefore, the results of Subczynski et al. suggest that an increase in cholesterol content can increase the partition coefficient by decreasing the hydrophobic barrier at the membrane surface, and decrease the rate of membrane transport by increasing the hydrophobic barrier in the hydrocarbon region. Thus, the fact that the permeability coefficient of DMA decreases with increasing cholesterol content implies that transmembrane permeation is, in this case, dominated by the hydrophobic core of the membrane.

The results reported here show that the major effect of cholesterol occurs at the 20% (mol) level, and that further increase in the cholesterol content has only a limited effect. Similar results have been observed by Demel et al. [32] and Subczynski et al. [43]. This behaviour is probably due to the balance between the increase in the partition coefficient and the decrease in the rate of membrane transport as cholesterol content is increased.

The activation energies observed in this work, for membranes free of cholesterol, are comparable to those observed for the permeability of a variety of charged and uncharged solutes [44]. The activation energy showed an initial increase upon the addition of $\approx 20\%$ cholesterol by mol. Further increases in the concentration of cholesterol in the membrane did not produce large increases in the activation energy; however, a trend toward higher values is seen. The observed activation energy is the sum of the $\Delta H^\circ$ of partitioning for DMA in the membrane and the activation energy of membrane translocation [45]

rendering any discussion on the effects of cholesterol qualitative until the separate values of $\Delta H^\circ$ (partition) and $E_a$ (translocation) are determined. Nonetheless, the dominant effect is expected to be in $E_a$.

Preexponential factors for the permeability of various solutes have not been widely studied, but variations are expected if permeation is an entropy-driven process [44]. Following a sharp increase in the Arrhenius preexponential factor after addition of about 20% cholesterol, a trend toward higher values was observed, paralleling cholesterol's effect on the activation energy. The widely varying permeabilities of both charged and neutral solutes and similarities of $E_a$ have led to the speculation that the selectivity of membrane transport is an entropy-driven process [44]. This speculation is not borne out in this work as we would expect a greater dependence of A on the cholesterol content. The subtlety of changes observed probably reflect the balance between the different physical–chemical properties of the surface and inner membranous regions.

## 5. Conclusions

The major impetus for this work is a better understanding of the bioavailability and bioaccumulation of the arsenicals DMA and MMA. The permeability coefficients for DMA are approximately two orders of magnitude larger than those for MMA. This result would lead to the prediction that a cell would be more likely to accumulate DMA than to MMA, if only passive diffusion of the neutral species were involved. This supposition is in agreement with earlier findings for *I. galbana*, *D. tertiolecta*, and *Candida humicola* [13]. If the rate-limiting step for the production of trimethylarsine (TMA) by *C. humicola* from either DMA or MMA is the diffusion of the substrate into the cell, then one would expect to see more TMA produced from DMA than from MMA, and this is in agreement with results described earlier [13]. The observed pH dependence on the rates of TMA production by *C. humicola* [13] may also be explained as the diffusion rates for both DMA and MMA increase with decreasing pH.

NMR spectroscopy can be used to measure permeability coefficients of hydrophilic compounds through LUVs. The technique has been applied to DMA and MMA where the effect of pH, cholesterol content, and temperature on the permeability is better understood. These coefficients can be used to make predictions concerning the biomobility and bioaccumulation of DMA and MMA. A simple consideration of their *n*-octanol/water partition coefficients, which have been shown to be similar [13], would have lead to erroneous conclusions. We intend to study the general applicability of these ideas with other important molecules.

## Acknowledgements

The Natural Sciences and Engineering Research Council of Canada (NSERC) is thanked for support in the form of research grants to F.G. Herring and W.R. Cullen and a postgraduate scholarship to R.G. Males. The University of British Columbia's Faculty of Science is thanked for financial support to P.S. Phillips.

## References

[1] B.E. Cohen, A.D. Bangham, Nature 236 (1972) 173.
[2] E. Orbach, A. Finkelstein, J. Gen. Physiol. 75 (1980) 427.
[3] A. Walter, J. Gutknecht, J. Membr. Biol. 90 (1986) 207.
[4] W.D. Stein, The movement of molecules across cell membranes, Academic Press, New York, 1967.
[5] J. de Gier, J.G. Mandersloot, J.V. Hupkes, R.N. McElhaney, W.P. Van Beek, Biochim. Biophys. Acta 233 (1971) 610.
[6] X. Chen, R.W. Gross, Biochemistry 33 (1994) 13769.
[7] G. Speelmans, R.W.H.M. Staffhorst, B. de Kruijff, F.A. de Wolf, Biochemistry 33 (1994) 13761.
[8] J. de Gier, J.G. Mandersloot, L.L.M. van Deenen, Biochim. Biophys. Acta 150 (1968) 666.
[9] F. Kamp, J.A. Hamilton, Biochemistry 32 (1993) 11074.
[10] J. Ko, J.A. Hamilton, H. Ton-Nu, C.D. Schteingart, A.F. Hofmann, D.M. Small, J. Lipid Res. 35 (1994) 883.
[11] P.R. Harrigan, K.F. Wong, T.E. Redelmeier, J.J. Wheeler, P.R. Cullis, Biochim. Biophys. Acta 1149 (1993) 329.
[12] F.G. Herring, W.R. Cullen, J.C. Nelson, P.S. Phillips, Bull. Magn. Res. 14 (1992) 289.
[13] W.R. Cullen, F.G. Herring, J.C. Nelson, Bull. Environ. Contam. Toxicol. 52 (1994) 171.
[14] L.O. Renberg, S.G. Sundstrom, A. Rosen-Olofsson, Toxicol. Environ. Chem. 10 (1985) 333.
[15] W.B. Neely, D.R. Branson, R.E. Blau, Environ. Sci. Technol. 8 (1974) 1113.
[16] M.T.M. Tulp, O. Hutzinger, Chemosphere 7 (1978) 849.
[17] A. Leo, C. Hansch, D. Elkins, Chem. Rev. 71 (1971) 525.

[18] J.M. Diamond, Y. Katz, J. Membr. Biol. 17 (1974) 121.
[19] W.R. Cullen, K.J. Reimer, Chem. Rev. 89 (1989) 713.
[20] A.K.Y. Tsang, The uptake of arsenicals by the marine algae *Isochrysis galbana* and *Dunaliella tertiolecta*, Masters Thesis, Univ. of British Columbia, Vancouver, Canada, 1990.
[21] W.R. Cullen, B.C. McBride, A.W. Pickett, Appl. Organomet. Chem. 4 (1990) 119.
[22] W.R. Cullen, J. Nelson, Appl. Organomet. Chem. 6 (1992) 179.
[23] R.G. Males, P.S. Phillips, F.G. Herring, Biophys. Chem. 70 (1998) 63–72.
[24] J.H. Prestegard, J.A. Cramer, D.B. Viscio, Biophys. J. 26 (1979) 575.
[25] K. Kirk, NMR Biomed. 3 (1990) 1.
[26] M.J. Hope, M.B. Bally, G. Webb, P.R. Cullis, Biochim. Biophys. Acta 812 (1985) 55.
[27] L.D. Mayer, M.J. Hope, P.R. Cullis, Biochim. Biophys. Acta 858 (1986) 161.
[28] C.H. Fiske, Y. Subbarow, J. Biol. Chem. 66 (1925) 375.
[29] D.S. Cafiso, W.L. Hubbell, Biophys. J. 39 (1982) 263.
[30] J. Gutknecht, A. Walter, Biochim. Biophys. Acta 649 (1981) 149.
[31] W.D. Stein, Channels, Carriers, and Pumps: An Introduction to Membrane Transport, Academic Press, CA, 1990.
[32] R.A. Demel, S.C. Kinsky, C.B. Kinsky, L.L.M. Van Deenen, Biochim. Biophys. Acta 150 (1968) 655.
[33] R.N. McElhaney, J. De Gier, E.C.M. Van der Neut-Kok, Biochim. Biophys. Acta 298 (1973) 500.
[34] B. Deuticke, C. Ruska, Biochim. Biophys. Acta 433 (1976) 638.
[35] M. Grunze, B. Forst, B. Deuticke, Biochim. Biophys. Acta 600 (1980) 860.
[36] M.H. Nouri-Sorkhabi, B.E. Chapman, D.R. Sullivan, P.W. Kuchel, Magn. Reson. Med. 32 (1994) 505.
[37] A.R. Waldeck, M.H. Nouri-Sorkhabi, D.R. Sullivan, P.W. Kuchel, Biophys. Chem. 55 (1995) 197.
[38] P.R. Cullis, FEBS Lett. 70 (1976) 225.
[39] R.A. Cooper, M.H. Leslie, S. Fischkoff, M. Shinitzky, S.J. Shattil, Biochemistry 17 (1978) 327.
[40] R.A. Cooper, J. Supramol. Struct. 8 (1978) 413.
[41] A.J. Robinson, W.G. Richards, P.J. Thomas, M.M. Hann, Biophys. J. 68 (1995) 164.
[42] H. Trauble, J. Membr. Biol. 4 (1971) 193.
[43] W.K. Subczynski, A. Wisniewska, J.J. Yin, J.S. Hyde, A. Kusumi, Biochemistry 33 (1994) 7670.
[44] G. Ceve, D. Marsh, Phospholipid Bilayers, Wiley, Toronto, Canada, 1987.
[45] A. Ono, S. Miyauchi, M. Demura, T. Asakura, N. Kamo, Biochemistry 33 (1994) 4312.